Nuclear Engineering and Technology 52 (2020) 1259–1265

Contents lists available at ScienceDirect

Nuclear Engineering and Technology

journal homepage: www.elsevier.com/locate/net

Original Article

Plastic scintillator beta ray scanner for in-situ discrimination of beta ray and gamma ray radioactivity in soil

Jun Woo Bae, Hee Reyoung Kim*

School of Mechanical, Aerospace and Nuclear Engineering, Ulsan National Institute of Science and Technology, UNIST-gil 50, Ulsan Metropolitan City, 44919, Republic of Korea

ARTICLE INFO

Article history:
Received 30 November 2018
Received in revised form
12 November 2019
Accepted 12 November 2019
Available online 14 November 2019

Keywords:
In-situ discrimination
Plastic scintillator
Residual radioactivity
Clearance level
^{90}Sr

ABSTRACT

A beta ray scanner was proposed for in-situ discrimination of beta and gamma ray radioactivity. This scanner is based on the principle that gamma and beta rays experience different changes in detection efficiency in scintillators with different geometries, especially with regard to the scintillator thickness. The ratios of the counting rates of gamma rays (R_{gamma}), beta rays (R_{beta}), and sample measurements (R_{total}) in a thick scintillator to those in a thin one are reported. The parameter X_{thick}, which represents the counting rate contributed by beta rays to the total counting rate in the thick scintillator, was derived as a function of those ratios. The values of R_{gamma} and R_{beta} for ^{60}Co and ^{90}Sr sources were estimated as 3.2 ± 0.057 and 0.99 ± 0.0049, respectively. The estimated beta ray contributions had relative standard deviations of 2.05–4.96%. The estimated range of the beta rays emitted from ^{90}Sr was 19 mm as per the Monte Carlo N-Particle simulation, and this value was experimentally verified. Homogeneous and surface contaminations of ^{60}Co and ^{90}Sr-^{90}Y were simulated for application of the proposed method. The counting rate contributed by the beta rays was derived and found to be proportional to the concentration of ^{90}Sr-^{90}Y contamination.

1. Introduction

Nuclear power plant sites can remain contaminated by radioactive nuclides, including long-lived beta emitters such as ^{90}Sr, even after their decommissioning and dismantling [1]. Therefore, these sites should be monitored before they are reopened to the public. To date, the radioactivity of contaminated soils has been analyzed in laboratories using liquid scintillation counters, inductively coupled plasma mass spectrometry, or gamma spectrometers. These methods provide precise and accurate radioactivity measurements [2,3]; however, they require substantial manpower and time for sampling contaminated samples and several pretreatment steps before analysis. Moreover, radioactivity analysis using liquid scintillation counters produces organic radioactive or non-radioactive waste that can cause secondary contamination [4]. The gamma ray dose rate or beta ray-based surface contamination of the site can be scanned by several commercialized devices [5]. The counting rates of beta rays can be measured in-situ at the soil surface using survey meters such as the Geiger–Müller counter; however, it is difficult to determine the type of particle being analyzed whether the counted particle is beta ray or not [6]. Discrimination between particle types is important for direct in-situ measurement of radiation in order to characterize the type or nuclide of the contaminant. Detectors that could be used to monitor alpha, beta, and gamma rays simultaneously have been developed but are not suitable for field measurements because they require implementation of multiple signal processing steps for pulse height analysis and experience the issue of overlap among counting rates measured for different particles [7–9]. Hence, in-situ and portable measurement devices for beta ray-emitting radionuclides are efficient for detecting radioactive hotspots (i.e., areas with high radioactive contamination) and facilitate the scanning of the entire site. Plastic scintillators are candidates for measuring beta rays as they are less sensitive to gamma rays and have the lowest density and effective atomic number of all solid scintillators [10,11]. The gamma ray sensitivity of a plastic scintillator varies according to its thickness; for example, the gamma ray sensitivity of a 1-mm planar type plastic scintillator is five times lower than that of its 5-mm counterpart [12]. These properties can be applied to the context in question; using a combination of scintillators, it is possible to scan beta rays while rejecting gamma rays.

* Corresponding author.
E-mail address: kimhr@unist.ac.kr (H.R. Kim).

https://doi.org/10.1016/j.net.2019.11.013

This study developed a scanning detector to measure and directly discriminate beta and gamma rays with better minimum detectable concentrations (MDCs) than conventional beta ray scanners. The developed detector comprised two plastic scintillators of different thicknesses. In this paper, we apply the theory of discrimination between beta and gamma rays to describe the development of the detector and a laboratory-scale performance test. For practical purposes, the efficiency and minimum detectable activity (MDA) were estimated using a Monte Carlo computational simulation. The definition of the effective volume (or mass) of the sample for in-situ measurements was also provided.

2. Materials and methods

2.1. Theory of beta and gamma ray discrimination

To discriminate beta and gamma rays in an arbitrary measurement, it is important to determine the ratio of beta rays to gamma rays. The beta ray counting rate can be easily obtained from the total counts if the fraction of the counts contributed by the beta rays is known. To calculate the contribution of beta radioactivity, the ratio of counting rates between the signals from a thick plastic scintillator and a thin one was used in this study. The counting rate decreases as the volume of the scintillator decreases. However, the degree of decrement is significantly different between beta and gamma rays because their mechanisms of energy loss differ. Beta radiation loses its energy continuously in a medium and is characterized by its stopping power, while gamma radiation loses its energy quickly by interacting with the medium [13].

Based on this principle, beta and gamma ray discrimination using the difference in gamma ray sensitivities of two planar plastic scintillators with different thicknesses was parameterized. The fraction of beta radiation can be determined from the ratio of counting rates between the scintillators of different thicknesses. The parameters X_{thick} and X_{thin} are hereby defined as the fraction of the beta ray counting rate to the total counting rate for the thick scintillator and its thin counterpart, respectively, as shown in Eqs. (1) and (2).

$$X_{Thick} = \frac{C_{beta,thick}}{C_{total,thick}} = \frac{C_{beta,thick}}{C_{beta,thick} + C_{gamma,thick}} \tag{1}$$

$$X_{Thin} = \frac{C_{beta,thin}}{C_{total,thin}} = \frac{C_{beta,thin}}{C_{beta,thin} + C_{gamma,thin}} \tag{2}$$

where $C_{beta,thick}$, $C_{gamma,thick}$, and $C_{total,thick}$ are the beta ray, gamma ray, and total counting rates for the thick plastic scintillator, respectively; and $C_{beta,thin}$, $C_{gamma,thin}$, and $C_{total,thin}$ are the corresponding parameters for the thin plastic scintillator. The counting rate ratio for the type of radiation p, R_p, is defined in Eq. (3).

$$R_p = \frac{C_{p,thick}}{C_{p,thin}} \tag{3}$$

In this formula, the subscript p can be substituted by *beta*, *gamma*, or *total*. The ratio between the two parameters, X_{thick} and X_{thin}, is derived in Eqs. (4) and (5).

$$\frac{X_{thin}}{X_{thick}} = \frac{C_{beta,thick} + C_{gamma,thick}}{C_{beta,thin} + C_{gamma,thin}} \times \frac{C_{beta,thin}}{C_{beta,thick}} = \frac{R_{total}}{R_{beta}} \tag{4}$$

$$\frac{1 - X_{thin}}{1 - X_{thick}} = \frac{R_{total}}{R_{gamma}} \tag{5}$$

Equations (4) and (5) are reduced to Eq. (6) for parameter X_{thick} as a function of each counting rate ratio.

$$X_{thick} = \frac{\frac{1}{R_{gamma}} - \frac{1}{R_{total}}}{\frac{1}{R_{gamma}} - \frac{1}{R_{beta}}} \tag{6}$$

where R_{gamma} is the ratio of the counting rate of the gamma rays between the thick and thin scintillators, R_{beta} is the ratio of the counting rate of the beta rays between the thick and thin scintillators, and R_{total} is the ratio of the total counting rate between the thick and thin scintillators.

Equation (6) implies that the beta ray contribution can be obtained by estimating R_{total}. R_{gamma} and R_{beta} for the detection system are estimated in the laboratory, and R_{total} is estimated by comparing the measured counting rate obtained from the detection systems of the thick and thin scintillators. The parameters R_{gamma} and R_{beta} were characterized with experiments, and the equations were used to derive the beta ray counting rate.

2.2. Uncertainty estimation

As several probabilistic variables existed in the parameter X_{thin}, the combined standard deviation of X_{thick} was calculated using the standard deviation for each variable in Eq. (6) [14].

$$\sigma(X_{thick}) = \sqrt{\left(\frac{\sigma\left(\frac{1}{R_{gamma}} - \frac{1}{R_{total}}\right)}{\frac{1}{R_{gamma}} - \frac{1}{R_{total}}}\right)^2 + \left(\frac{\sigma\left(\frac{1}{R_{gamma}} - \frac{1}{R_{beta}}\right)}{\frac{1}{R_{gamma}} - \frac{1}{R_{beta}}}\right)^2} \times X_{thick} \tag{7}$$

2.3. Experimental setup for characterization of the proposed method

The developed system consists of a plastic scintillator, photomultiplier tube (PMT), PMT base with a preamplifier, high-voltage power supply, main amplifier, and multi-channel analyzer. The two scintillators were commercially supplied by EPIC Crystal Co. Ltd. Each scintillator was attached to the window of the PMT (R878, Hamamatsu Photonics) using optical cement (BC-600, Saint-Gobain Crystals). Both scintillators were circular plates with diameters of 50 mm each and thicknesses of 1 mm and 10 mm. The PMT was mounted on the PMT base with a preamplifier (276, Ortec Inc.) and a sufficiently high voltage of +1250 V was supplied using a high voltage power supply (556, Ortec Inc.). The signal was amplified by a spectrometer amplifier (855, Ortec Inc.) and collected by a multichannel analyzer (EASY-MCA-2k, Ortec Inc.).

Radioactive disc sources (RSS3 Disk Source Sets, Spectrum Techniques) were located 100 mm away from the plastic scintillator. The labelled activities were 3.7 kBq and 37 kBq for the ^{90}Sr and ^{60}Co sources, respectively. Before using the sources, all activities of the sources were corrected to account for the radioactive

Table 1
Summary of source sets and their radioactivities used in the experiments.

Source ID	Source Description
Sr	6.9 kBq (^{90}Sr-^{90}Y)
Co	27 kBq (^{60}Co)
SrCo	6.9 kBq (^{90}Sr-^{90}Y), 27 kBq (^{60}Co)
SrCoCo	6.9 kBq (^{90}Sr-^{90}Y), 27 & 18 kBq (^{60}Co)
SrSrCo	6.9 & 6.5 kBq (^{90}Sr-^{90}Y), 27 kBq (^{60}Co)

decay and equilibrium. Table 1 summarizes the source sets and their radioactivities used for the experiments. Each measurement was conducted for 600 s. Fig. 1 presents the conceptual diagram and photograph of the experimental system used in this study. Two PMTs were bundled and fixed. Although the heights of the scintillators differed, a support fixture was used to level them with the end of the detector.

Equation (8) was used to estimate the counting efficiency.

$$\varepsilon\ (\%) = \frac{\textit{Net Counting Rate}\ [\text{cps}]}{\textit{Disintegration Per Second}\ [\text{Bq}]} \times 100 \tag{8}$$

In the case of the ^{90}Sr source, disintegration was considered for the radioactivities of both ^{90}Sr and ^{90}Y.

Fig. 2 shows the experimental setup used to estimate the beta ray transmission characterization according to the thickness of the soil. Typical garden soil was used in the experiment, and the apparent density of the soil was measured to be 0.60 ± 0.02 g/cm^3. In general, soil density has been reported to range from values as small as 0.33 g/cm^3 to values as large as 1.3 g/cm^3 [15,16]. This difference reflects variations in soil depth and properties such as its water content. The density of surface soil bulk is low, making it suitable for surface scanning experiments.

A plastic scintillator-based detector assembly was used to measure the beta rays. The plastic scintillator of 12 mm (Φ) × 20 mm (H) was coupled with an optical guide of 100 mm (Φ) × 20 mm (H), which was then optically coupled with the PMT surface. A compact PMT socket with a signal processor (digiBASE, Ortec Inc.) was used to provide the power supply and conduct electronic signal processing. A^{90}Sr source was inserted in the soil and placed at a distance of 0–22 mm from the detector. In all the experimental procedures, the scintillator and detector were flushed with nitrogen gas to minimize the measurement error due to contamination.

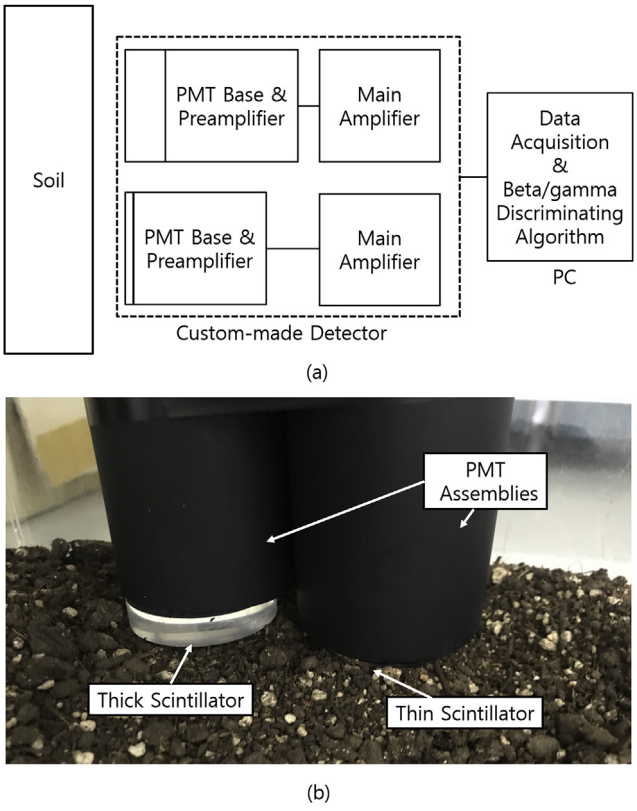

Fig. 1. (a) Conceptual diagram and (b) photograph of the custom-made detector.

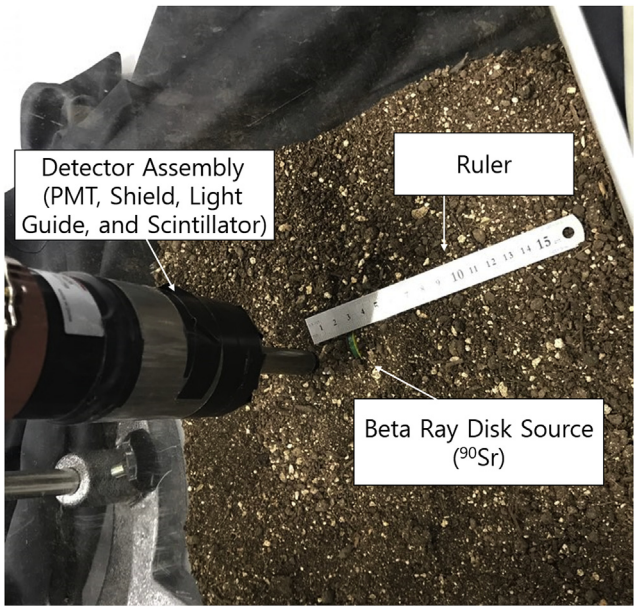

Fig. 2. Experimental setup for estimation of beta ray transmission characterization according to the thickness of the soil.

2.4. Monte Carlo simulation for estimation of minimum detectable activity

The International Atomic Energy Agency's Safety Standards Series No. Rs-G-1.7 [17] specifies the concentrations of various radionuclides for clearance. The concentration of ^{90}Sr for unconditional release of a site is 1 Bq/g. The ^{90}Sr-^{90}Y beta ray energy spectrum was carefully emulated using physical data provided by Report 56 of the International Commission on Radiation Units and Measurements [18].

As homogeneous radioactive soil samples are difficult to prepare, Monte Carlo N-Particle (MCNP) simulations were carried out to estimate the range of ^{90}Sr beta rays in homogeneously contaminated soil. Fig. 3 shows the simulation geometry used to estimate the efficiency and effective detection range of the detector for the contaminated soil using the MCNP simulation, which is a general Monte Carlo-based radiation transport code [19]. The contamination depth, *T*, was varied from 0 to 22 mm, and the soil was assumed to be contaminated homogeneously at all selected depths. While estimating the detectable range of contamination in the soil, it was assumed that the soil was contaminated homogeneously for the same diameter as that of the scintillator. The density

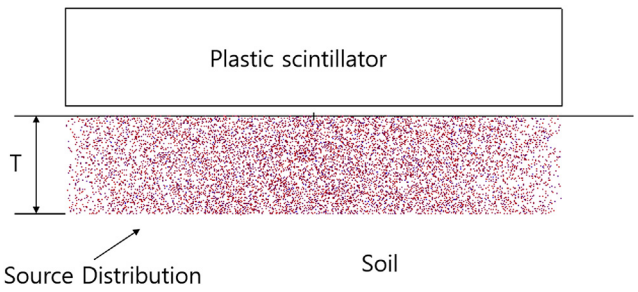

Fig. 3. Simulation geometry to estimate the efficiency of the detector for the contaminated soil.

of the soil was the same as that used in the experiment (i.e., 0.6 g/cm^3), and the composition of the soil was the same as that used by Wielopolski et al. [20].

Given the above information, it was expected that the counting rate would increase before the depth of contamination became less than the range of the beta rays. However, the contamination depth, which was greater than the range of the beta rays, was impossible to detect; thus, the counting rate did not increase further and was saturated.

The maximum depth of the soil for which the beta rays could be detected was determined to define the effective volume of soil to be used in the estimation of the MDA. The MDA was estimated in terms of Currie's MDA for a single measurement, as described in Eq. (9) [14]:

$$\mathrm{MDA}\left[\frac{\mathrm{Bq}}{\mathrm{g}}\right] = \frac{2.71 + 4.65\sqrt{B}}{T \cdot V \cdot \varepsilon \cdot K} \tag{9}$$

where B is the background count during the measurement time, T; V is the sample volume or mass; ε is the detection efficiency; and K is the recovery factor, which accounts for the decrease in radioactivity due to radioactive decay. The recovery factor was not considered in this study because the detection system was used to measure in-situ radiation directly.

2.5. Monte Carlo simulation to validate the proposed method

The proposed method was computationally simulated with two types of soil contamination: homogeneous contamination and surface contamination. For homogeneous contamination, the defined contaminated area measured 40 × 40 cm and its depth was 50 cm. The area for the surface contamination was the same, but the depth of the contamination was defined as 5 cm; that is, the surface contamination of ^{90}Sr was distributed mainly between 0 and 5 cm in the soil [21]. Although few studies have reported contamination depths higher than 5 cm for ^{90}Sr [22], the range of the beta rays indicates that higher depths would not affect the simulation or measurement results. The ^{60}Co gamma ray and ^{90}Sr-^{90}Y beta ray cases were carefully emulated based on the ICRU report [2]. Both contamination cases were simulated, and the suitability of the proposed method was estimated. To emulate the site with a mixed source, two different concentrations of site status were assumed. The radioactive concentration of one site was defined as 0.2 Bq/g of ^{60}Co and 1 Bq/g of ^{90}Sr-^{90}Y, and that of the other was defined as 0.1 Bq/g of ^{60}Co and 2 Bq/g of ^{90}Sr-^{90}Y. The number of particles used in the simulation was 10^7, and the uncertainty of the simulation results was maintained to below 0.1%.

Table 2
Counting rates for two different scintillators (thick and thin) according to the sources.

Data ID		Counting Rates (cpm)
Thick	BKG	$8.03 \times 10^2 \pm 1.17 \times 10^1$
	Co	$4.20 \times 10^3 \pm 4.65 \times 10^1$
	Sr	$6.87 \times 10^3 \pm 2.35 \times 10^1$
	SrCo	$1.04 \times 10^3 \pm 7.88 \times 10^0$
	SrCoCo	$1.32 \times 10^3 \pm 1.87 \times 10^1$
	SrSrCo	$1.71 \times 10^4 \pm 3.02 \times 10^1$
Thin	BKG	$3.98 \times 10^2 \pm 8.43 \times 10^0$
	Co	$1.48 \times 10^3 \pm 9.06 \times 10^0$
	Sr	$6.56 \times 10^3 \pm 1.19 \times 10^1$
	SrCo	$7.65 \times 10^3 \pm 5.99 \times 10^1$
	SrCoCo	$8.03 \times 10^3 \pm 4.00 \times 10^1$
	SrSrCo	$1.34 \times 10^4 \pm 6.16 \times 10^0$

3. Results

3.1. Measured results and estimation of parameters

Table 2 presents the counting rates of five source sets and the background. The represented counting rates were calculated by subtracting the background counting rate from the measured counting rate for each source set. For the thick scintillator, the detection efficiencies for ^{90}Sr and ^{60}Co were estimated as 1.5 and 0.21%, respectively. Notably, the arrangement was geometrically efficient (the source and the scintillator were 100 mm apart and the diameter of the scintillator was 50 mm), and the solid angle was approximately 0.03. The respective intrinsic efficiencies were estimated as 49 and 7.0%. For the thin scintillator, the detection efficiencies for ^{90}Sr and ^{60}Co were estimated as 1.5 and 0.067%, and the intrinsic efficiencies were 50 and 2.2%, respectively. Compared to the thick plastic scintillator, the estimated efficiencies for beta ray detection were very similar, with a relative difference of 1.5%, but those for the gamma ray detection were three times higher. The ratios of the counting rates between the thick and thin scintillators (corresponding to the values of R_{total}) are listed in Table 3. Additionally, the counting rates due to the beta rays were estimated using Eq. (1). The standard deviations of the estimated counting rates were carefully derived based on the principle of error propagation using Eq. (7). The relative errors of the estimated counting rates compared with one ^{90}Sr source were 0.46, 0.77, and 1.13%. The corresponding relative standard deviations of the estimated counting rates were 3.54, 4.97, and 2.06% (i.e., lower than 5%). The counting rate ratios (R_{gamma} and R_{beta}) obtained from the measurements of the other sets of radiation sources were characterized, and the contributions of the beta and gamma rays were discriminated with relative standard deviations lower than 5%.

In the case of SrCo, the average counting rates matched the sum of the independent counting rates for a single ^{90}Sr or a single ^{60}Co source. The dead time of the detector was negligible because the decay time of plastic scintillators is, in general, a few nanoseconds, which is shorter than the decay time of the PMT, while the transient time of the R878 model is 70 ns [23].

3.2. Characterization of effective volume

Fig. 4 shows the normalized counting rates according to the distance between the detector and a^{90}Sr source in the soil, which were estimated via the simulation and measured experimentally. Both counting rates were normalized at a distance of 0 mm. The results were used to estimate the effective distance in the soil at which the detector could detect signals from the beta rays. The maximum distance of beta ray detection was estimated to be 19 mm for the ^{90}Sr/^{90}Y beta ray case by the MCNP simulation. It was difficult to define the maximum distance of beta ray detection by the experimental method because the thickness and density of the soil were difficult to control, and a number of counts included statistical errors. Thus, the distance was approximated and compared with the simulation result. The experimental results showed the net counting rates for soil thicknesses of 19 and 22 mm to be 5.2 ± 4.9 and 3.4 ± 6.2 cpm, respectively. These net counting rates were considered as the background levels, because the relative standard deviation of them were 94 and 182%, respectively. There were no meaningful beta ray counts after 19 mm of soil covered over the source. Additionally, the thickness of 19 mm is reasonable by comparing with the MCNP simulation results. Therefore, the detectable range of the beta rays was defined as 19 mm.

The diameter of the plastic scintillator based on the proposed detector design was 50 mm, and considering that the range of beta

Table 3
Estimated parameters using the measured counting rates of the thick and thin scintillators.

Data ID	Ratio of Counting Rates Between Thick and Thin Scintillators (R_{total})	Beta Ray Counting Fraction (X_{thick})	Estimated Counting Rates Due to Beta Rays (cpm)
Co	$3.2 \times 10^{0} \pm 5.7 \times 10^{-2}$	0.0×10^{0}	N/A
Sr	$9.9 \times 10^{-1} \pm 4.9 \times 10^{-3}$	1.0×10^{0}	$6.1 \times 10^{3} \pm 9.8 \times 10^{1}$
SrCo	$1.3 \times 10^{0} \pm 1.1 \times 10^{-2}$	6.3×10^{-1}	$6.0 \times 10^{3} \pm 2.1 \times 10^{2}$
SrCoCo	$1.6 \times 10^{0} \pm 8.1 \times 10^{-3}$	4.7×10^{-1}	$6.0 \times 10^{3} \pm 3.0 \times 10^{2}$
SrSrCo	$1.2 \times 10^{0} \pm 2.6 \times 10^{-3}$	7.7×10^{-1}	$1.2 \times 10^{4} \pm 2.4 \times 10^{2}$

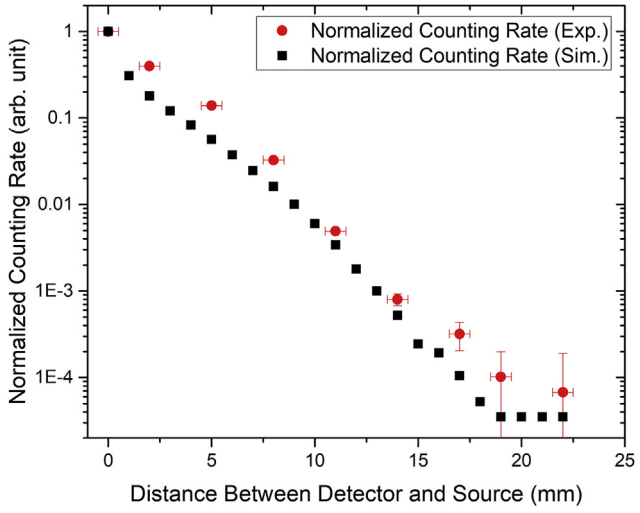

Fig. 4. Normalized counting rate according to the distance between the detector and a ^{90}Sr source in the soil.

ray detection was 19 mm, the effective source volume was estimated to be 37.3 cm^3. The density of the soil was 0.60 g/cm^3, and the activity of the contaminated soil at 19 mm of depth was 22.4 Bq. In this case, the detection efficiency of the plastic scintillator was estimated to be 4.2% by the MCNP simulation. In practical applications, this value should be estimated more carefully because additional factors, such as optical loss, photon-electron conversion efficiency, background counting rate fluctuation due to random noise, and soil conditions, can reduce the detection efficiency. Note that the efficiency estimated by the simulation was used for predicting the expected MDA. For practical application, soil characterization for each site was carried out first, and the detection efficiency of the detector was calibrated carefully to estimate the MDA correctly.

3.3. Estimation of minimum detectable activity

Table 4 shows the estimated MDA of ^{90}Sr/^{90}Y for various measurement times. The background counting rate was 13.4 cps. An MDA of 1.0 Bq/g was possible for a measurement time of 335 s. For scanning of radioactive contaminated field, it is recommended that the MDA be lower than one-tenth of the target radioactivity [24]. An MDA of 0.1 Bq/g was achievable for a measurement time of 33,100 s. Hence, the detection system can be used for continuous environmental monitoring for measurement times longer than 33,100 s, and for quick monitoring of residual radioactivity for measurement times longer than 335 s. As the purpose of in-situ measurement is rapid characterization, the measurement result should consider the approximate radioactivity level of the soil. Considering that the relative standard deviations estimated in this study were lower than 5%, radioactive hotspots can be identified using this method. Using our result as the MDC for surficial scanning, a value of 34 dpm/100 cm^2 was acquired for a detection time of 2 min.

3.4. Application to two types of contamination

Table 5 provides a summary of the estimated detection efficiencies according to the types of contamination, scintillators, and particles. Three types of particles were used (^{60}Co gamma and beta rays, and ^{90}Sr-^{90}Y beta rays). The detection efficiency for the ^{60}Co beta rays was relatively lower than those for the ^{60}Co gamma rays and ^{90}Sr-^{90}Y beta rays.

Tables 6 and 7 show the parameters and counting rates for the beta rays estimated with the proposed method for homogeneous and surface contamination, respectively. A small fraction of the counting rate due to the beta rays was included for the contamination of ^{60}Co with a concentration of 0.1 Bq/g. In this case, X_{thick} was only 0.00364. In the case of the combined contamination, namely 0.2 Bq/g of ^{60}Co and 1 Bq/g of ^{90}Sr, and 0.1 Bq/g of ^{60}Co and 2 Bq/g of ^{90}Sr), the values of X_{thick} were 0.373 and 0.703, respectively. These values were proportional to the concentration of ^{90}Sr-^{90}Y in the soil. The trend for the surface contamination was the same as that for the homogeneous contamination.

The relative errors between the combined source and only the ^{90}Sr-^{90}Y cases were less than 1%. Although this was a small error, it was caused by the beta rays of ^{60}Co. This error can be corrected if a detection efficiency calibration database for general beta decay radionuclides (i.e., excluding the pure beta-emitting nuclides) is created. It is important to accurately characterize this effect especially when the nuclides emits high-energy beta rays followed by gamma rays (e.g., ^{137}Cs).

4. Discussion

A ^{90}Sr/^{90}Y source was used as an example for MDA estimation with the proposed detector. ^{90}Sr/^{90}Y is considered to be the main pure beta-emitting radionuclide in soil at decommissioning sites. This example showed that a counting time of 335 s was sufficient to yield an MDA of 1.0 Bq/g, which is equal to the release criterion for a decommissioning site. The MDCs of conventional Geiger–Müller counters and gas proportional counters for ^{90}Sr and ^{90}Y are 550 and 170 dpm/100 cm^2, respectively [24]. The proposed detector showed an MDC of 34 dpm/100 cm^2, which is considerably lower than those of conventional detectors. The relative errors estimated in this

Table 4
Estimated MDA of ^{90}Sr/^{90}Y for various measurement times with the detection system.

Time (s)	Detection Limit (Counts)	MDA (Bq/g)
60	$1.3 \times 10^{2} \pm 2.1 \times 10^{-1}$	$2.4 \times 10^{0} \pm 3.7 \times 10^{-3}$
300	$3.0 \times 10^{2} \pm 4.7 \times 10^{-1}$	$1.1 \times 10^{0} \pm 1.7 \times 10^{-3}$
335	$3.1 \times 10^{2} \pm 5.0 \times 10^{-1}$	$1.0 \times 10^{0} \pm 1.6 \times 10^{-3}$
1,800	$7.2 \times 10^{2} \pm 1.2 \times 10^{0}$	$4.3 \times 10^{-1} \pm 6.8 \times 10^{-4}$
3,600	$1.0 \times 10^{3} \pm 1.6 \times 10^{0}$	$3.0 \times 10^{-1} \pm 4.9 \times 10^{-4}$
28,800	$2.9 \times 10^{3} \pm 4.6 \times 10^{0}$	$1.1 \times 10^{-1} \pm 1.5 \times 10^{-4}$
33,100	$3.1 \times 10^{3} \pm 4.9 \times 10^{0}$	$1.0 \times 10^{-1} \pm 1.8 \times 10^{-4}$

Table 5
Simulated detection efficiencies according to the types of contamination, scintillators, and particles (^{60}Co gamma rays and beta rays, and ^{90}Sr-^{90}Y beta rays).

Contamination Type	Scintillator	Particle Type	Detection Efficiency
Homogeneous Contamination	**Thick**	^{60}Co (gamma)	1.10×10^{-3}
		^{60}Co (beta)	4.02×10^{-6}
		^{90}Sr-^{90}Y (beta)	1.30×10^{-4}
	Thin	^{60}Co (gamma)	1.59×10^{-4}
		^{60}Co (beta)	3.48×10^{-6}
		^{90}Sr-^{90}Y (beta)	9.06×10^{-5}
Surface Contamination	**Thick**	^{60}Co (gamma)	4.34×10^{-3}
		^{60}Co (beta)	4.07×10^{-5}
		^{90}Sr-^{90}Y (beta)	1.16×10^{-3}
	Thin	^{60}Co (gamma)	6.95×10^{-4}
		^{60}Co (beta)	3.36×10^{-5}
		^{90}Sr-^{90}Y (beta)	8.63×10^{-4}

Table 6
Simulated counting rate ratios (R_{gamma}, R_{beta}, and R_{total}), portion of counting rate due to beta rays to the total counting rate (X_{thick}), and estimated count rates due to beta rays by applying the proposed method for homogeneous contamination.

Radioactivity Concentration of Source (Bq/g)	0.1 ^{60}Co (Bq/g)	1 ^{90}Sr (Bq/g)	0.2 ^{60}Co & 1 ^{90}Sr (Bq/g)	1.1 ^{60}Co & 2 ^{90}Sr (Bq/g)
R_{gamma}	6.94			
R_{beta}	1.44			
R_{total}	6.82	1.44	2.86	1.88
X_{thick}	3.64×10^{-3}	1.00	3.73×10^{-1}	7.03×10^{-1}
Total Counting Rate (cps)	5.31	6.25	16.9	17.8
Estimated Counting Rate due to Beta Rays (cps)	$\mathbf{1.93 \times 10^{-2}}$	**6.25**	**6.30**	**12.5**

Table 7
Simulated counting rate ratios (R_{gamma}, R_{beta}, and R_{total}), portion of counting rate due to beta rays to the total counting rate (X_{thick}), and estimated count rates due to beta rays by applying the proposed method for surface contamination.

Radioactivity Concentration of Source	0.1 ^{60}Co (Bq/g)	1 ^{90}Sr (Bq/g)	1.2 ^{60}Co & 1 ^{90}Sr (Bq/g)	1.1 ^{60}Co & 2 ^{90}Sr (Bq/g)
R_{gamma}	6.25			
R_{beta}	1.34			
R_{total}	6.02	1.34	2.02	1.53
X_{thick}	1.10×10^{-2}	1.00	5.74×10^{-1}	8.43×10^{-1}
Total Counting Rate (cps)	2.09	5.56	9.77	13.2
Estimated Counting Rate due to Beta Rays (cps)	$\mathbf{2.22 \times 10^{-2}}$	**5.56**	**5.61**	**11.2**

study were lower than the values obtained using the Phoswich detector for simultaneous alpha/beta/gamma ray measurement. In the latter case, the overlapping portion between the alpha and beta rays was 7.1% and that between the beta and gamma rays was 8.1% [7]. It is considered that the proposed detection technique could overcome the underestimation of pure beta emitters, which is encountered when using conventional detectors.

The following aspects merit careful consideration for practical use. First, several conditions related to field application should be considered. The proposed detector was designed as an integrated beta and gamma ray scanner to optimize radioactivity scanning tasks, which consume considerable time and resources. Nuclear instrument modules have been used for accurate measurements in laboratories; however, as demonstrated by this study, an integrated PMT base with MCA (digiBASE, Ortec Inc.) can be used for field applications. Second, the equipment used in this study did not include a protector as we wanted to avoid contamination and ensure the highest detection efficiency; it is inappropriate to use a fully closed protector as the beta rays are to be transmitted. To protect the scintillator from contamination, a net-shaped grid can be arranged on the front face of the scintillator. The aspect ratio of the grid should be small because the loss in detection efficiency due to both blocking by the grid and the short range of beta rays should be considered. The detection efficiency should be re-estimated when the grid is applied. Although the use of a grid can reduce the detection efficiency, it is expected to be effective as errors due to contamination and failure will be reduced. It is possible to prevent damaging or contaminating the scintillator due to direct contact; however, fine dust particles will likely cause some issues. To reduce the error due to contamination, washing using an air gun can be considered. Third, the estimation efficiency of the MDA should be considered for practical usage. The detector should be calibrated in the same way as a beta ray scanner or gamma ray detector. A homogeneous volumetric source or surficial source can be used. Fourth, the manufacture of homogenous radioactive soil source is expected to pose some difficulties. However, the proposed detector can be employed using conservative criteria for the detection limit of the counting rate. Fifth, before applying this method in the field, simulations and MDA calculations should be carried out according to the site to be characterized, because the characteristics of the soil (e.g., mineral composition, density, and water content) may differ from those considered in this study. The parameters may change slightly for beta and gamma rays of various energies. In the case of beta rays, sensitivities do not vary significantly, except in the case of very high energy rays, but in the case of gamma rays, the counting rate varies exponentially with respect to the gamma ray linear attenuation coefficient. Thus, this value may vary depending on the energy. However, this study focused on discriminating beta and gamma rays and preventing undervaluation of pure beta-emitting nuclides according to their counting rate. It was theoretically and experimentally verified that this method can be applied to practical cases even though certain parameters

may change. Sixth, in this study, a soil density of 0.60 g/cm^3 was used. Because the efficiencies obtained from the MCNP simulation results and the experimental results were similar, we believe that the density chosen for this study was appropriate. If, for example, a higher soil density is used, the detection efficiency would decrease, resulting in a greater MDA, because the effective volume of the soil becomes smaller. Thus, when characterizing sites for decommissioning nuclear power plants, the historical data of the site should be used. Accordingly, all relevant geological information should be collected, analyzed, and applied to correct the effective volume.

5. Conclusion

A method for discrimination of beta and gamma rays was presented for in-situ measurements of residual radioactivity. The method was verified using both a customized scintillator-based radiation detector and MCNP simulations. The experimental results showed the feasibility of in-situ measurements and discrimination of beta and gamma rays with a tolerable relative error and standard deviation. The instrument developed in this study is able to simultaneously measure and distinguish between beta and gamma rays. The expected MDA of the developed detector satisfies the clearance level mandated by the International Atomic Energy Agency standard for decommissioning sites. Furthermore, it has a lower MDC than conventional beta ray scanners. Hence, this method can be used to effectively detect high contamination levels of beta ray-emitting radionuclides in the soil as well as radiation emergencies/accidents at nuclear power facilities. The proposed method can be effectively applied to in-situ measurements of beta rays if a low-power and coincidence circuit is used to reduce the background counting rate. A system with a lower MDC or MDA will be developed in the future to measure environmental levels of radioactivity.

Acknowledgements

This work was supported in part by the “Development of the Beta ray Distribution Measurement Technology of the Site” through the Ministry of Education of the Republic of Korea and the Korea Atomic Energy Research Institute under Grant KAERI-2015-2015M2A8A5022235, in part by the Industrial Technology Innovation Program (Real-Time Underwater Tritium Monitoring Technology by Electrolysis) through the Korea Institute of Energy Technology Evaluation and Planning under Grant 2016520101340, and in part by the National Research Foundation of Korea through the Korean Government (MSIP: Ministry of Science, ICT and Future Planning) under Grant 2016M2B2B1945083.

References

[1] D.K. Cho, H.J. Choi, R. Ahmed, G. Heo, Radiological characteristics of decommissioning waste from a CANDU reactor, Nucl. Eng. Technol. 43 (2011) 583–592.
[2] M.F. L'Annunziata, Handbook of Radioactivity Analysis, Vol third ed, Academic Press, Amsterdam, 2012, pp. 576–609.
[3] C. Miro, A. Baeza, M.J. Madruga, R. Perianez, Caesium-137 and strontium-90 temporal series in the Tagus river: experimental results and a modelling study, J. Environ. Radioact. 113 (2012) 21–31.
[4] H. Miyoshi, T. Ikeda, Preparation of paper scintillator for detecting H-3 contaminant, Radiat. Prot. Dosim. 156 (2013) 277–282.
[5] C.H. Shao, C.C. Lu, T.R. Chen, J.H. Weng, P.F. Kao, S.L. Dong, M.J. Chou, Monitoring of radiation dose rates around a clinical nuclear medicine site, Radiat. Phys. Chem. 104 (2014) 124–128.
[6] H. Cember, Introduction to health physics, McGraw-Hill, Health Professions Division, New York; London, 1996, pp. 432–434.
[7] S. Usuda, H. Abe, A. Mihara, Simultaneous counting of alpha-rays, beta rays and gamma rays with phoswich detectors, J. Alloy. Comp. 213 (1994) 437–439.
[8] S. Yamamoto, J. Hatazawa, Development of an alpha/beta/gamma detector for radiation monitoring, Rev. Sci. Instrum. 82 (2011) 113503.
[9] K. Yasuda, S. Usuda, H. Gunji, Simultaneous alpha, beta/gamma, and neutron counting with phoswich detectors by using a dual-parameter technique, IEEE Trans. Nucl. Sci. 48 (2001) 1162–1164.
[10] E. Furuta, T. Kawano, A plastic scintillation counter prototype, Appl. Radiat. Isot. 104 (2015) 175–180.
[11] T. Maekawa, S. Makino, A. Sumita, T. Goto, Long scintillation detector using composite light guide for beta ray survey measurement, J. Nucl. Sci. Technol. 48 (2011) 50–59.
[12] T. Maekawa, A. Sumita, S. Makino, Thin beta ray detectors using plastic scintillator combined with wavelength-shifting fibers for surface contamination monitoring, J. Nucl. Sci. Technol. 35 (1998) 886–894.
[13] International Commission on Radiation Units and Measurements, Stopping powers for electrons and positrons, in: International Commission on Radiation Units and Measurements, 1984.
[14] G.F. Knoll, Radiation Detection and Measurement, Wiley, Hoboken, N.J, 2010, pp. 85–92.
[15] T.J. Yasunari, A. Stohl, R.S. Hayano, J.F. Burkhart, S. Eckhardt, T. Yasunari, Cesium-137 deposition and contamination of Japanese soils due to the Fukushima nuclear accident, Proc. Nat.Acad. Sci. 108 (49) (2011) 19530–19534.
[16] J.C. Callaway, R.D. DeLaune, W.H. Patrick Jr., Chernobyl 137Cs used to determine sediment accretion rates at selected northern European coastal wetlands, Limnol. Oceanogr. 41 (3) (1996) 444–450.
[17] International atomic energy agency, Application of the Concepts of Exclusion, Exemption and Clearance, IAEA Safety Standards Series No. RS-G-1.7, IAEA, Vienna, 2004, pp. 12–15.
[18] W.G. Cross, J. Böhm, M. Charles, E. Piesch, S.M. Seltzer, Report 56: dosimetry of external beta rays for radiation protection, Rep. Int. Comm. Radiat. Units Meas. os29 (1) (1997) 107–109, 5 January.
[19] U.A. Tarim, O. Gurler, E.N. Ozmutlu, S. Yalcin, Monte Carlo calculations for gamma ray mass attenuation coefficients of some soil samples, Ann. Nucl. Energy 58 (2013) 198–201.
[20] L. Wielopolski, Z. Song, I. Orion, A.L. Hanson, G. Hendrey, Basic considerations for Monte Carlo calculations in soil, Appl. Radiat. Isot. 62 (2005) 97–107.
[21] B.L. Rosenberg, et al., Radionuclide pollution inside the Fukushima Daiichi exclusion zone, part 1: depth profiles of radiocesium and strontium-90 in soil, Appl. Geochem. 85 (2017) 201–208.
[22] L.M. Kagan, V.B. Kadatsky, Depth migration of Chernobyl originated 137Cs and 90Sr in soils of Belarus, J. Environ. Radioact. 33 (1) (1996) 27–39.
[23] K.K. Hamamatsu Photonics, Photomultiplier tubes: photomultiplier tube and related products, 2016, pp. 44–45.
[24] E.W. Abelquist, W.S. Brown, G.E. Powers, A.M. Huffert, Minimum detectable concentrations with typical radiation survey instruments for various contaminants and field conditions (NUREG-1507), in: U.S. Nuclear Regulatory Commission, Washington D. C, 1998, pp. 4–9.